

Image pattern recognition by edge detection using discrete wavelet transforms

Ravikant Divakar¹, Bijenda Singh¹, Ashish Bajpai¹ and Anil Kumar^{1,*}

¹ Department of Physics, Hindu College, Moradabad, Affiliated to M.J.P. Rohilkhand University, Bareilly, India

* Correspondence: akumarmbd@gmail.com

Received 3 July 2021

Accepted for publication 16 April 2022

Published 29 April 2022

Abstract

An edge is the high-frequency part of an image and represents the location where abrupt changes take place in the intensity of luminescence. Edge detection is a basic step in feature extraction and pattern recognition of any image. Wavelet transforms extract low- and high-frequency information from any signal separately. In a two-dimensional wavelet transformation, an image is decomposed into four sub-images: one approximation image and three different images (horizontal, vertical, and diagonal images) at each decomposition level. The difference images show how the neighboring pixels differ in the horizontal, vertical, and diagonal directions. The approximation coefficients are forced to zero, and the difference coefficients are inverse wavelet transformations, as the reconstructed image shows the edges of the image and describes its pattern. Using the Haar wavelet at decomposition levels 1, 2, and 3, image pattern recognition by edge detection is performed and discussed.

Keywords: edge, image, approximation, difference, Haar, wavelet.

1. Introduction

Edge is the line that develops understanding about the image; therefore, the image without edge does not make sense to the eyes. An edge is defined as a location in an image where the luminescence level or gray level changes abruptly (Canny, 2010). Edges are actually high frequencies in an image. It marks the boundary of discontinuity or strong contrast in luminescence in an image. Edge detection is a fundamental step in image analysis and machine vision systems; it analyses an image by identifying edges in an image or visual data. Edge detection is a pattern recognition problem to an extent and is very challenging. Edge detection is a very important technique in computer and machine vision and has wide applications in biometric recognition, automatic character recognition, document processing, remote sensing, medical imaging, surveillance, automotive sensing, human-computer interaction, visual inspection, etc. Edge detection precedes image segmentation and feature extraction stages in image analysis and also acts as a dimensionality reduction technique in feature extraction. In this sense, only relevant features in an image sufficient to identify the image are extracted while redundant features are discarded. Several classical edge detectors have been used for detecting edges in images (Aydin et al., 1996). These operators work based on thresholding the pixels within a specified window. An operator may take the average value of pixels within a window as the threshold and may be likened to an averaging filter. The

threshold then depends on the presence, absence and the value of the pixels within that window. These classical edge detectors have limitations in detecting edges in noisy and faint images. Meaningful and spurious edges are likely to be detected in a noisy image while edges could be omitted in a faint image, hence, classical operators cannot adequately analyse noisy images. Most signals encountered in life, in real-time (audio, video, image, motion, pressure) have some degree of noise; hence, a reliable edge detection technique should be sensitive to edges and insensitive to noise (Wei et al., 2009).

Fourier transform is well known technique of spectral analysis in which trigonometrical functions of various periods are used to represent functions at various scales. The techniques of Fourier analysis are powerful and find wide ranging applications not only in mathematical sciences but also in physics and engineering. From a statistical point of view, obtaining the Fourier spectrum of a function is the same as obtaining the least square fit of sines and cosines of various frequencies in one or more dimensions. Multiple regression using trigonometrical functions is very elegant and simple. The trigonometrical sines and cosines are mutually orthonormal, and the Fourier coefficients are written as simple sum of products (in the discrete case) or as integral of products of functions (in the continuous case). This process is called Fourier transformation (Hernandez and Weiss, 1996). Fourier transform plays an important role in the theory of many branches of science. A waveform optical, electrical, or acoustical and its spectrum are appreciated equally as physical pictorial and measurable entities: an oscilloscope enables us to see optical or electrical spectra. Our acoustical appreciation is even more direct, since ear hears spectra. Waveform and spectra are Fourier transform of each other; the Fourier transform is thus an eminent physical relationship. The principle of phase contrast microscope is reminiscent of the circuit for detecting frequency modulation, and the explanation of both is conveniently, given in terms of transforms along the same line. It is well known that the response of a system is itself harmonic at the same frequency to harmonic input, under two conditions: linearity and time invariance of the system.

Wavelets were introduced in the beginning of the 1980s. The formalization and emergence of wavelet theory is the result of multidisciplinary efforts of Mathematicians, Physicists and Engineers. The transient's world is considerable larger and more complex than the garden of stationary signals. In wavelet theory, the functions/signals are expressed as the superposition of simple and fixed building blocks at different positions and scales. Wavelets have been found quite useful in image edge detection. In discrete wavelet transform (DWT) the varying of the time resolution and frequency resolution (scaling) properties are achieved with the use of filters (high-pass and low-pass) and sub-sampling respectively. Scaling is achieved by successively passing the input signal through half-band cut-off low-pass and high-pass filters and sub-sampling the outputs of both filters (Soman and Ramchandran, 2005). In 2D-DWT, the transform is first applied to the columns of the image which consistently halves the sizes of all columns in the image and then applied to the rows in like manner. The resultant image would be reduced or sub-sampled by 4. Haar wavelets decompose an image of size $N \times M$ into four sub-images of sizes $N/2 \times M/2$, where N and M are even. The decomposed images are the approximation image A (LL), horizontal H (HL), vertical V (LH), and diagonal D (HH) differences' images (Alarcon-Aquino et al., 2013; Decoster et al., 2000). The differences' images show how the neighbouring pixels differ in the vertical, horizontal and diagonal directions. A two level Haar decomposition of an image gives rise to approximations (A_1 and A_2) as well as details ($H1, H2, V1, V2, D1, D2$) images. Edges can be found in regions of high contrast; therefore, more attention was given to the coefficients derived from high-pass filtering of the image.

2. Literature review

Fourier transform gives the spectrum of any time invariant signal having finite energy. However, the Fourier transform of a time varying signal does not register frequencies with time. For getting time localization of spectral characteristics of a time varying signal, a window function is introduced into Fourier analysis. Window Fourier atoms were introduced in 1946 by Gabor to measure localized frequency components of sound. A signal is multiplied by a window function and thereafter its Fourier transforms is taken, so that the spectral information of the signal to the domain of influence of the window function are obtained. The window function is translated over the time axis to cover the entire time domain, and the spectral information of signal localized neighbourhood in time is obtained (Antoine, 1999). This transform is called the window Fourier transform (WFT) or short time Fourier transform (STFT). From Heisenberg uncertainty principle, the resolution in time and frequency cannot be taken accurately and simultaneously, so that the signal is treated as small bursts associated with long quasi stationary components, and each component is analysed with good time resolution or frequency resolution, but not both. It is necessary to be able to localize high frequency transient spectral information to a relatively narrow time interval while allowing a relatively a wider time interval to identify low frequency characteristics in order to capture complete information. In other words, it is desirable to be able to zoom in on the signal for identifying short duration transients corresponding to high frequency bursts (Heil and Walnut, 1989).

Wavelet is the function exhibiting oscillatory behaviour for a short time interval and then dies out. For any two real numbers a and b , a wavelet function is defined as (Wickerhauser, 1994; Prasad and Iyenger, 1997):

$$\psi_{a,b}(t) = \frac{1}{\sqrt{a}} \psi\left(\frac{t-b}{a}\right) = T_b D_a \psi \quad (1)$$

Putting $a = 2^{-j}$ and $\frac{b}{a} = k$, we get discrete wavelets as following:

$$\psi_{j,k}(t) = 2^{j/2} \psi(2^j t - k) \quad (2)$$

where a and b are the dilation and translation parameter respectively. Here $\psi(t)$ is real-valued and this collection of wavelets is used as an orthonormal basis.

The continuous wavelet transform is the modified WFT and defined as:

$$W_{a,b} = \int f(t) \frac{1}{\sqrt{a}} \psi\left(\frac{t-b}{a}\right) dt \quad (3)$$

The discrete wavelet transform is defined as:

$$W_{j,k} = \int f(t) 2^{j/2} \psi(2^j t - k) dt \quad (4)$$

2.1 Multiresolution analysis (MRA)

An MRA is a new recursive method to perform the discrete wavelet transforms (Mallat, 1989; Daubechies, 1990; Rioul and Vetterli, 1991; Coifman and Wickerhauser, 1992). It consists of a sequence $V_j : j \in \mathbb{Z}$ of closed subspaces of Lebesgue space $L^2(\mathbb{R})$, a space of square integrable functions, satisfying the properties as follows:

- 1) $V_{j+1} \subset V_j : j \in \mathbb{Z}$,
- 2) $\bigcap_{j \in \mathbb{Z}} V_j = \{0\}$, $\bigcup_{j \in \mathbb{Z}} V_j = L^2(\mathbb{R})$,
- 3) For every, $L^2(\mathbb{R})$, $f(t) \in V_j \Rightarrow f(2t) \in V_{j+1}$, $\forall j \in \mathbb{Z}$.
- 4) There exists a function $\phi(t) \in V_0$ such that $\{\phi(t - k) : k \in \mathbb{Z}\}$ is orthonormal basis of V_0 .

The function $\phi(t)$ is called scaling function of given MRA and property 3 implies a dilation equation as follows:

$$\phi(t) = \sum_{k \in \mathbb{Z}} h_k \sqrt{2} \phi(2t - k) \quad (5)$$

where h_k is low pass filter and is defined as:

$$h_k = \left(\frac{1}{\sqrt{2}}\right) \int_{-\infty}^{\infty} \phi(t)\phi(2t - k) dt \tag{6}$$

Now we consider W_1 be orthogonal compliment of V_1 in V_0 i.e.

$$V_0 = V_1 \oplus W_1$$

If $\psi \in W_1$ be any wavelet function then

$$\psi(t) = \sum_{k \in \mathbb{Z}} g_k \sqrt{2} \phi(2t - k) \tag{7}$$

where $g_k = (-1)^{k+1} h_{1-k}$ are high pass filters. In general, we can write,

$$V_j = V_{j+1} \oplus W_{j+1} \tag{8}$$

But,

$$V_{j+1} = V_{j+2} \oplus W_{j+2}$$

Therefore,

$$\begin{aligned} V_j &= W_{j+1} \oplus W_{j+2} \oplus V_{j+2} \\ &\quad \dots \quad \dots \quad \dots \\ V_j &= W_{j+1} \oplus W_{j+2} \oplus W_{j+3} \oplus \dots \oplus W_{j+p} \oplus V_{j+p} \end{aligned} \tag{9}$$

where p is any desired number representing the order of level of decomposition.

2.2 One dimensional (1D) wavelet transform

A function f (that is for which $\int_{\mathbb{R}} |f(x)| dx < \infty$) has a wavelet series expansion in vector space V_j ,

$$f(x) = \sum_{k \in \mathbb{Z}} a_{j+p,k} \phi(x - k) + \sum_{p=1}^{\infty} \sum_{k \in \mathbb{Z}} d_{j+p,k} \psi_{j+p,k}(x) \tag{10}$$

It also follows that the sum $\sum_{k \in \mathbb{Z}} a_{j+p,k} \phi(x - k)$ is the orthogonal projection of f on the space V_{j+p} of square integrable functions that are constant on integer end point intervals $[k, k + 1)$. For $j = 0$, the sum $\sum_{p=1}^{\infty} \sum_{k \in \mathbb{Z}} d_{j+p,k} \psi_{j+p,k}(x)$ adds the details required to obtain an approximation in the space V_p of square integrable functions that are constant on all intervals.

If all such functions u and v are orthogonal ($\langle u, v \rangle = 0$), then W_j is the orthogonal complement of V_j in V_{j-1} ($V_j \perp W_j$) and the construction below will give the scaling function and mother wavelet of an orthonormal wavelet basis for $L^2(\mathbb{R})$. By MRA, the orthogonal decomposition of p th level of space V_j is as following:

$$V_j = V_{j+p} \oplus \sum_{p=1}^{\infty} W_{j+p}$$

A discrete signal is approximated in space of square summable sequences $\ell^2(\mathbb{Z})$ as follows (Kumar et al., 2015; Kumar et al., 2021):

$$f[n] = \frac{1}{\sqrt{M}} \sum_k a[j + p, k] \phi_{j+p,k}[n] + \frac{1}{\sqrt{M}} \sum_{p=1}^{\infty} \sum_k d[j + p, k] \psi_{j+p,k}[n] \tag{11}$$

Here $f[n]$, $\phi_{j+p,k}[n]$ and $\psi_{j+p,k}[n]$ are discrete functions defined in $[0, M - 1]$, totally M points. Because the sets $\{\phi_{j+p,k}[n]\}_{k \in \mathbb{Z}}$ and $\{\psi_{j+p,k}[n]\}_{k \in \mathbb{Z}, p \in \mathbb{Z}^+}$ are orthogonal to each other. The We wavelet coefficients can be obtained by taking the inner product as follows:

$$a[j + p, k] = \frac{1}{\sqrt{M}} \sum_n f[n] \phi_{j+p,k}[n] \tag{12}$$

$$d[j + p, k] = \frac{1}{\sqrt{M}} \sum_n f[n] \psi_{j+p,k}[n] \tag{13}$$

where $a[j + p, k]$ and $d[j + p, k]$ are called approximation and detailed coefficients respectively. From property of scaling function,

$$\begin{aligned}\phi_{j,k}[n] &= 2^{j/2} \phi[2^j n - k] \\ &= 2^{j/2} \sum_{n'} h[n'] \sqrt{2} \phi[2(2^j n - k) - n'] \\ &= 2^{(j+1)/2} \sum_{n'} h[n'] \phi[2^{(j+1)} n - 2k - n']\end{aligned}$$

Let $n' = m - 2k$, we have $\phi_{j,k}[n] = 2^{(j+1)/2} \sum_m h[m - 2k] \phi[2^{(j+1)} n - m]$. Now the approximation coefficient,

$$\begin{aligned}a[j, k] &= \frac{1}{\sqrt{M}} \sum_n f[n] \phi_{j,k}[n] \\ &= \frac{1}{\sqrt{M}} \sum_n f[n] 2^{j/2} \phi[2^j n - k] \\ &= \frac{1}{\sqrt{M}} \sum_n f[n] 2^{j/2} \sum_m h[m - 2k] \sqrt{2} \phi[2^{j+1} n - m] \\ &= \sum_m h[m - 2k] \left(\frac{1}{\sqrt{M}} \sum_n f[n] 2^{j+1/2} \phi[2^{j+1} n - m] \right) \\ &= \sum_m h[m - 2k] a[j + 1, n] \\ &= \sum_{n'} h[n'] * a[j + 1, n], \text{ where } k \geq 0.\end{aligned}$$

Similarly, for the detail coefficients, it is,

$$a[j, k] = g[n'] * d[j + 1, n], \text{ where } k \geq 0.$$

By taking $j = 0$, we get,

$$\begin{aligned}a[0, k] &= \sum_{n'} h[n'] * a[1, n] \\ a[0, k] &= g[n'] * d[1, n] \text{ where } k \geq 0.\end{aligned}$$

2.3 Two dimensional (2D) wavelet transforms

Digitization is a process in which an analogue image $a(x, y)$ in a 2D continuous space is converted into a digital image $a[m, n]$ described in a 2D discrete space through a sampling process (Gangetto et al., 2006). In an image, the intersection of a row and a column is called a pixel. The value assigned to the integer coordinates $[m, n]$ with $\{m = 0, 1, 2, \dots, M - 1\}$ and $\{n = 0, 1, 2, \dots, N - 1\}$ is $a[m, n]$, where M and N are rows and columns of 2D continuous image $a(x, y)$ respectively. In 2D wavelet transform, the scaling and wavelet function are two variable functions denoted as $\phi(x, y)$ and $\psi(x, y)$. The dilated and translated basis functions are defined as follows:

$$\begin{aligned}\phi_{j,m,n}(x, y) &= 2^{j/2} \phi(2^j x - m, 2^j y - n) \\ \psi_{j,m,n}^i(x, y) &= 2^{j/2} \psi^i \phi(2^j x - m, 2^j y - n), i = \{1, 2, 3\}\end{aligned} \quad (14)$$

The $\psi^i(x, y)$ represent three different wavelet functions, $\psi^1(x, y)$, $\psi^2(x, y)$ and $\psi^3(x, y)$ (Santhosh et al., 2012). However, the wavelet function is related to the order to apply the filters. The functions can be easily rewritten as,

$$\begin{aligned}\phi(x, y) &= \phi(x)\phi(y) \\ \psi^1(x, y) &= \psi(x)\phi(y) \\ \psi^2(x, y) &= \phi(x)\psi(y) \\ \psi^3(x, y) &= \psi(x)\psi(y)\end{aligned}$$

The analysis and synthesis equations in 2D wavelet transforms are modified to,

$$\begin{aligned}a[j + p, m, n] &= \frac{1}{\sqrt{MN}} \sum_{x=0}^{M-1} \sum_{y=0}^{N-1} f(x, y) \phi_{j+p,m,n}(x, y) \\ d^i[j + p, m, n] &= \frac{1}{\sqrt{MN}} \sum_{x=0}^{M-1} \sum_{y=0}^{N-1} f(x, y) \psi_{j+p,m,n}^i(x, y)\end{aligned}$$

where $i = \{1, 2, 3\}$. Therefore, a two-dimensional signal can be defined in terms of wavelet coefficients as follows

$$\begin{aligned}f(x, y) &= \frac{1}{\sqrt{MN}} \sum_m \sum_n a[j + p, m, n] \phi_{j+p,m,n}(x, y) \\ &\quad + \frac{1}{\sqrt{MN}} \sum_{i=1,2,3} \sum_{p=1}^{\infty} \sum_m \sum_n d^i[j + p, m, n] \psi_{j+p,m,n}^i(x, y)\end{aligned} \quad (15)$$

3. Research methodology

A two-dimensional wavelet transform is the superposition of two separate one-dimensional wavelet transforms. First of all, the adaptive and best wavelet is selected for the given image, that is Haar wavelet (Kharate et al., 2007; Kumar, 2017). Thereafter the image is filtered along x -dimension through low pass analysis filters and thereafter through high pass analysis filters and decimated by two. Low pass filtered wavelet coefficients are stored on the left part of the matrix and high pass wavelet filtered coefficients on the right. The decimation process is applied to maintain size of the transformed image same as the size of original image (Figure 1).

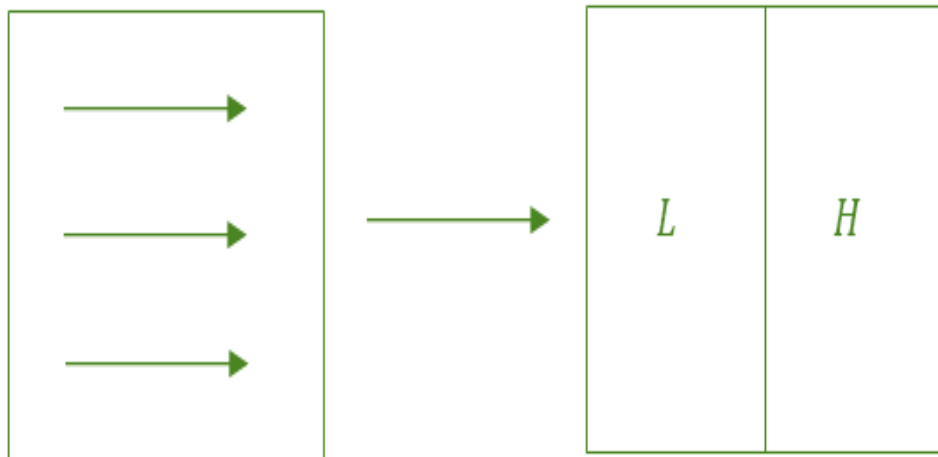


Figure 1. Horizontal transform; 2 sub-band

Then, filtering the sub-image is performed along the y -dimension and decimated by two. Finally, after first level decomposition, the image is divided into four sub-bands denoted by $LL1$, $HL1$, $LH1$, and $HH1$ (Figure 2).

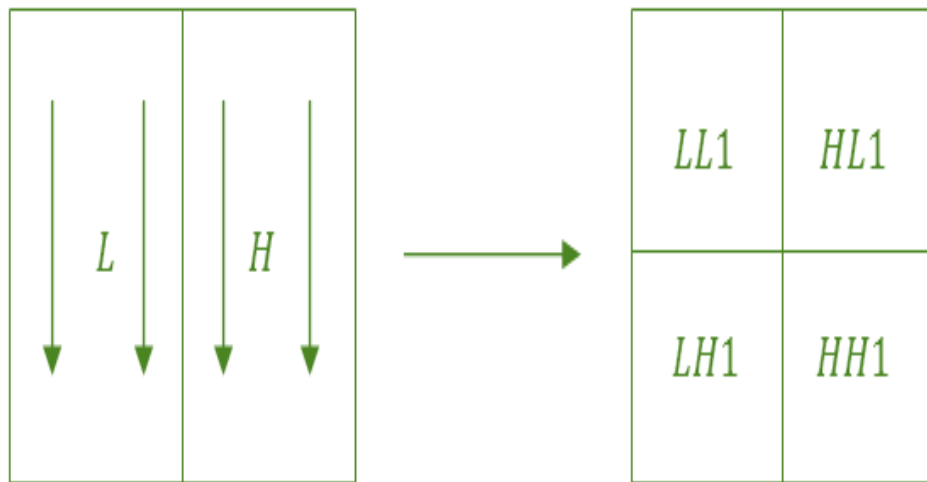


Figure 2. Vertical transform; 4 sub-bands

The process of filtering the image is called pyramidal decomposition of the image. With help of 2D-wavelet transform of an image, the scaling and wavelet functions can be described as,

$$\begin{aligned}\phi_{j,m,n}(x,y) &= 2^{j/2}\phi(2^jx - m, 2^jy - n) \\ \psi_{j,m,n}^i(x) &= 2^{j/2}\psi^i(2^jx - m, 2^jy - n),\end{aligned}$$

for $1 \leq i \leq 3$. The wavelet functions $\{\psi_{j,m,n}^1, \psi_{j,m,n}^2, \psi_{j,m,n}^3\}$ form an orthonormal basis of the subspace of details,

$$W_j^2 = (V_j \otimes W_j) (W_j \otimes V_j) \oplus (W_j \otimes W_j)$$

at scale j . The Lebesgue space $L^2(\mathbb{R}^2)$ can be expressed as

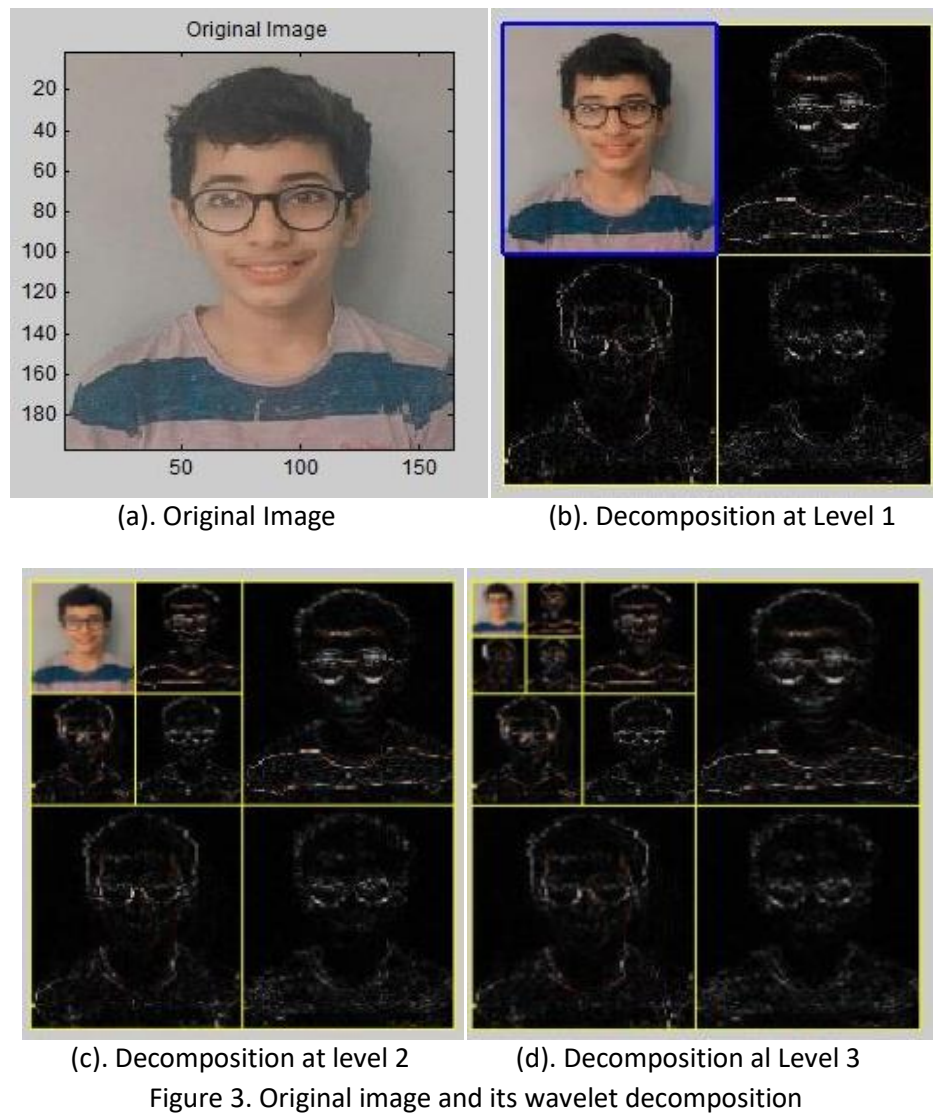
$$L^2(\mathbb{R}^2) = \sum_{\oplus_j} W_j^2 \quad (16)$$

Discrete wavelet transforms with a cascade of filtering with \bar{h} and \bar{g} is followed by sub-sampling by a factor of 2. The $LL1$, $HL1$, $LH1$ and $HH1$ are each $M/2 \times N/2$ submatrices. The trend $LL1$ consists of scaling coefficients, whereas the fluctuations $HL1$, $LH1$ and $HH1$ consist of wavelet coefficients for each of the three kinds of wavelet basis functions. The trend $LL1$ contains scaling coefficients for the scaling basis $\{\phi_{j,M-1}(x)\phi_{k,M-1}(y)\}$ and occupies the upper left quadrant of the transform. In each step of decomposition, the scaling coefficients of the image is decomposed to the next level of decomposition. This process is continuously going on until the required level of decomposition is achieved using MATLAB toolbox (Pratap, 2006).

The left most three plots $LL1$, $LL2$, $LL3$ represent approximation of the image at level 1, 2 and 3 respectively. Similarly, from top to bottom next to it are horizontal details (representing horizontal edges) $HL1$, $HL2$, $HL3$ represent horizontal details, $LH1$, $LH2$, $LH3$ represent vertical details, and $HH1$, $HH2$, $HH3$ represent diagonal details respectively. The approximation represents lower frequencies and details (or edges) higher frequencies. The approximation coefficients are forced to zero in the required level of decomposition. For edge detection, the image is reconstructed with help of detail coefficients. We have chosen Haar wavelet as an adaptive and best wavelet for the wavelet transforms of the image at decomposition level 1, 2 and 3.

4. Results and discussion

Original image of a child is taken as a raw image (figure 3(a)). The wavelet approximation and detailed coefficients are determined with help of 2D wavelet transform using Haar wavelet, level-1, 2 and 3. The wavelet transformed images at level 1 are shown in figure 3(b). Image of Left upper corner represents approximated version of the image corresponding to the lower frequencies, while other three images represent its detailed version corresponding to the higher frequencies. Image of right upper corner shows horizontal edges, left lower image to the vertical edges and right lower images to the diagonal edges. Similarly, the wavelet transformed images at level 2 (Figure 3(c)) and at level 3 (Figure 3(d)) represent second and third order edges corresponding to lower and higher frequencies. The trend LL consists of scaling coefficients is clearly a low pass version and HL , LH & HH consist of wavelet coefficients are clearly high pass version of the original image.



It is clear from the wavelet analysis that lower frequency version of the image represents trend of the images, while high frequency version represents edges of the image horizontally, vertically and diagonally. Now the wavelet coefficients corresponding to lower frequencies at decomposition level 3 are forced to zero and inverse wavelet transform of wavelet coefficients corresponding to higher frequencies are performed. We find pattern of the image with edge detection (Figure 4).



Figure 4. Image Pattern with Edge Detection

5. Conclusion

The wavelet transforms using multiresolution analysis decomposes a signal into average and detail coefficients corresponding to lower and high frequencies respectively. The 2-D wavelet transforms perform average and difference between pixel values to form the approximation and detail coefficients of an image. At the edges of an image the luminescence changes abruptly and correspond to the high frequencies' locations. Haar wavelet is optimum and best wavelet for the considered image. The image pattern recognition with edge detection is performed at decomposition level 3 through excluding the approximation version of the image. SEM, TEM and other images can be well analysed by this discrete wavelet transform technique. Therefore, this method of edge detection is very useful in surface morphological study of samples in material science and especially in nanotechnology.

References

- Alarcon-Aquino, V., Ramirez-Cortes, J. M., Gomez-Gil, P., Starostenko, O., & Lobato-Morales, H. (2013). Lossy image compression using discrete wavelet transform and thresholding techniques. *The Open Cybernetics & Systemics Journal*, 7, 32-38.
- Antoine, J. P. (1999). Wavelet analysis: A new tool in Physics. In: Van Den Berg, J.C. (ed) *Wavelets in Physics*. (pp. 9-22). Cambridge: Cambridge University Press.
- Aydin, T., Yemez, Y., Anarim, E., & Sankur B. (1996). Multidirectional and multiscale edge detection via M-band wavelet transform. *IEEE Transactions on Image Processing*, 5(9), 1370-1377.
- Canny, J. (2010). A computational approach to edge detection. *IEEE Transactions on Pattern Analysis and Machine Intelligence*, 8(6), 679-698.
- Coifman, R. R., & Wickerhauser, M. V. (1992). Entropy based algorithms for best basis selection. *IEEE Transactions on Information Theory*, 38(2), 713-718.
- Daubechies, I. (1990). The wavelet transforms, time frequency localization and signal analysis. *IEEE Transaction on Information Theory*, 6, 961 – 1005.
- Decoster, N., Roux, S. G., & Ameodo A. (2000). A wavelet-based method for multifractal image analysis. *European Physical Journal B*, 15(4), 739-764.
- Gangetto, M., Magli, E., Martina, M., & Olmo, G. (2006). Optimization and implementation of the integer wavelet transform for image coding. *IEEE Transactions on Image Processing*, 11(2), 596-604.
- Heil, C., & Walnut, D. (1989). Continuous and discrete wavelet transforms. *SIAM review*, 31, 628-666.

- Hernandez, E., & Weiss, G. (1996). *A First Course on Wavelets*. New York: CRC Press.
- Kharate, G. K., Patil, V. H., & Bhale, N. L. (2007). Selection of mother wavelet for image compression on basis of nature of image. *Journal of Multimedia*, 2(6), 44-51.
- Kumar, A. (2017). Selection of optimal base wavelet for image compression. *World Journal of Engineering, Research and Technology*, 3(4), 396-405.
- Kumar, A., Kumar, S., & Pathak, J. K. (2015). Spectral analysis of river Ramganga hydraulics using discrete wavelet transform. *Proceedings of International Conference of Advance Research and Innovation (ICARI 2025)*, 370-373.
- Kumar, A., Singh R., & Kumari, M. (2021). Spectral analysis of human face expressions and behaviour using wavelet transforms. *Design Engineering*, 21(4), 1628-1636.
- Mallat, S. G. (1989). A theory for multiresolution signal decomposition: The wavelet representation. *IEEE Transactions on Pattern Analysis and Machine Intelligence*, 11, 674-693.
- Prasad, L., & Iyenger, S. S. (1997). *Wavelet Analysis with Application to Image Processing*. New York: CRC Press.
- Pratap, R. (2006). *Getting Started with MATLAB7*, 2nd Ed. Delhi: Oxford University Press.
- Rioul, O., & Vetterli, M. (1991). Wavelets and signal processing. *IEEE Signal Processing Magazine*, 8(4), 14-38.
- Santhosh, M., Charles, B. S., & Prasad M. N. G. (2012). Adaptive filter design for wavelet decomposition and reconstruction in image processing applications. *ARNP Journal of Engineering and Applied Sciences*, 7(3), 314-318.
- Soman, K. P. K., & Ramchandran I. (2005). *Insight into Wavelets: From Theory to Practice*. 2nd ed. Delhi: Prentice Hall of India.
- Wickerhauser, M.V. (1994). *Adaptive Wavelet Analysis from Theory to Software*. Wellesley: A.K. Peters Limited.
- Wei, J., Kin-Man L., & Ting-Zhi, S. (2009). Efficient Edge Detection Using Simplified Gabor Wavelets. *IEEE Transactions on Systems, Man, and Cybernetics, Part B: Cybernetics*, 39(4), 1036-1047.